BIOCHEMISTRY
including biophysical chemistry & molecular biology

Article

pubs.acs.org/biochemistry

A tRNA-Dependent Two-Enzyme Pathway for the Generation of Singly and Doubly Methylated Ditryptophan 2,5-Diketopiperazines

Tobias W. Giessen, Alexander M. von Tesmar, and Mohamed A. Marahiel*

Department of Chemistry and LOEWE-Center for Synthetic Microbiology, Philipps-University, Hans-Meerwein-Strasse-4, 35032 Marburg, Germany

Supporting Information

ABSTRACT: A large number of bioactive natural products containing a 2,5-diketopiperazine (DKP) moiety have been isolated from various microbial sources. Especially tryptophan-containing cyclic dipeptides (CDPs) show great structural and functional diversity, while little is known about their biosynthetic pathways. Here, we describe the bioinformatic analysis of a cyclodipeptide synthase (CDPS)-containing gene cluster from *Actinosynnema mirum* spanning 2.9 kb that contains two putative DKP-modifying enzymes. We establish the biosynthetic pathway leading to two methylated ditryptophan CDPs through *in vivo* and *in vitro* analyses. Our studies identify the first CDPS (Amir_4627) that shows high substrate specificity synthesizing only one main product, cyclo(Trp-Trp) (cWW). It is the first member of the CDPS family that can form ditryptophan DKPs and the first prokaryotic CDPS whose main product constituents differ from the four amino acids (Phe, Leu, Tyr, and Met) usually found in CDPS-dependent CDPs. We show that after cWW formation a *S*-adenosyl-L-methionine-dependent *N*-methyltransferase (Amir_4628) conducts two successive methylations at the DKP-ring nitrogens and additionally show that it is able to methylate four other phenylalanine-containing CDPs. This makes Amir_4628 the first identified DKP-ring-modifying methyltransferase. The large number of known modifying enzymes of bacterial and fungal origin known to act upon Trp-containing DKPs makes the identification of a potent catalyst for cWW formation, encoded by a small gene, valuable for combinatorial *in vivo* as well as chemoenzymatic approaches, with the aim of generating derivatives of known CDP natural products or entirely new chemical entities with potentially improved or new biological activities.

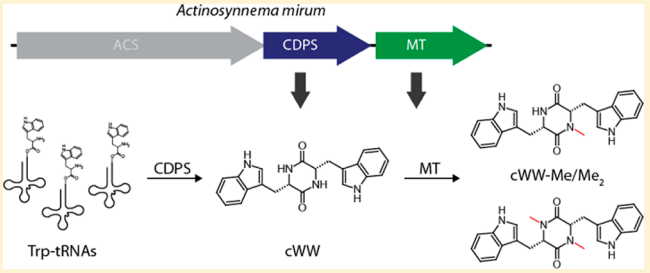

A large number of 2,5-diketopiperazine (DKP)-containing natural products have been isolated from microbial sources, and many have received an increased level of attention in recent years because of their diverse and interesting biological activities, ranging from antibacterial[1,2] and immunosuppressive[3] to antineoplastic.[4,5] In general, the DKP-ring system is formed through the condensation of two amino acids resulting in the smallest possible cyclic peptide and has long been recognized as a privileged structural scaffold in the search for new synthetic or semisynthetic pharmacologically useful compounds.[6] With regard to the physiological function of CDPs in the respective producing organisms, only a limited amount of information is available that indicates a function in biochemical communication phenomena like intra- and intercellular signaling[7,8] and quorum sensing.[9,10]

Tryptophan (Trp)-containing CDPs are among the most prevalent DKP-containing natural products and have been isolated from a diverse range of microbial sources, among them many different *Aspergillus* and *Penicillium* species.[6] In contrast, comparatively few Trp-containing CDPs of bacterial origin are known.[6] Tryptophan residues that are part of a DKP can exist in a monocyclic form like most other amino acids or in an annulated form in which an additional five-membered ring is generated through formation of a bond between the α-nitrogen and the indole C2 of the Trp residue resulting in a tetracyclic (6−5−5−6) ring system (Figure 1A).[6] A large majority of DKP natural products that contain two Trp residues are annulated, while only a small number of monocyclic ditryptophan DKPs could be isolated so far, namely, the fellutanins from *Penicillium fellutanum*,[11] Sch 725418 from *Micromonospora* sp.,[12] and a number of okaramine congeners from *Penicillium simplicissimum* (Figure 1A).[13]

From a biosynthetic standpoint, it has long been known that nonribosomal peptide synthetases (NRPSs) are able to generate DKP-containing compounds, either through a dedicated pathway or through the premature release of peptidyl intermediates via cyclization.[14−16] With the discovery of the albonoursin biosynthetic gene cluster in *Streptomyces noursei* and the characterization of the first cyclodipeptide synthase (CDPS) AlbC, a second unrelated pathway exclusively dedicated to the formation of CDPs could be identified.[17,18] CDPSs are able to form two successive peptide bonds in an ATP-independent fashion by hijacking aminoacyl-tRNAs (aa-tRNAs) from the ribosomal machinery and directly using them as substrates for the generation of a DKP-ring system (Figure 1B).[19] Putative CDPS-

Received: April 17, 2013
Revised: May 24, 2013
Published: May 24, 2013

   dx.doi.org/10.1021/bi4004827 | *Biochemistry* 2013, 52, 4274−4283

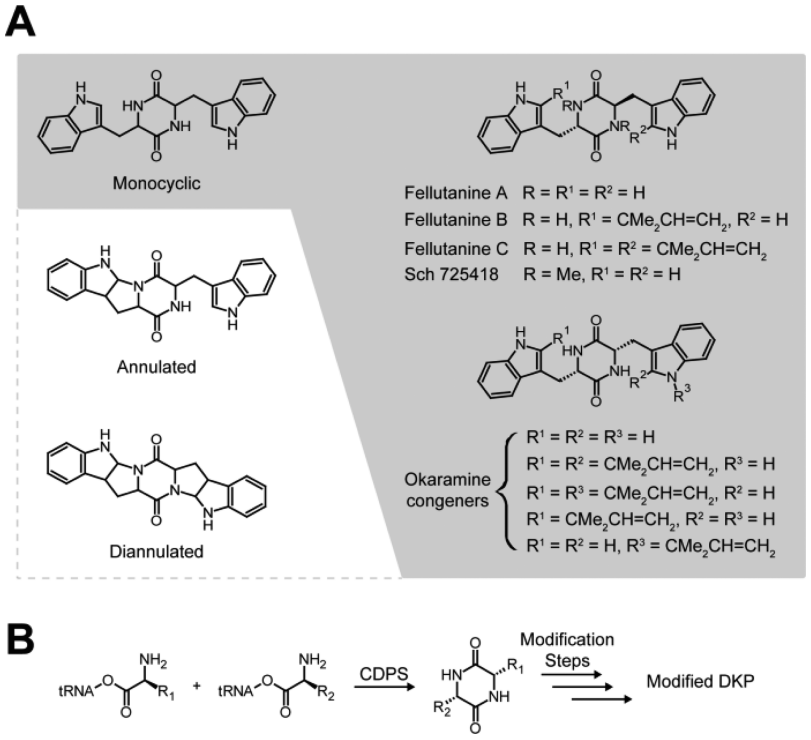

Figure 1. Overview of ditryptophan DKPs and CDPS-catalyzed reactions. (A) General structures of monocyclic, annulated, and diannulated ditryptophan DKPs. Additionally, all known monocyclic ditryptophan DKP natural products are shown highlighted with a gray background. (B) CDPSs use aa-tRNAs as substrates to generate a 2,5-DKP that is usually further modified by at least one tailoring enzyme found in the respective CDPS gene cluster.

encoding genes have been found through the use of iterative PSI-BLAST searches in many prokaryotic and a few eukaryotic species, amounting to more than 50 putative gene clusters in total.[20,21] To date, all biochemically characterized CDPSs have been shown to possess a certain degree of substrate promiscuity, usually generating a number of different CDP products. In prokaryotes, all main products consist of different combinations of the four amino acids phenylalanine, leucine, tyrosine, and methionine, while the only characterized eukaryotic CDPS mainly generates cyclo(Trp-Xaa) (cWX), with Xaa being one of the four previously mentioned amino acids.[21,22] In the direct surroundings of all putative prokaryotic CDPS genes, at least one, but oftentimes more than one, putative DKP-modifying enzyme can be found, including cytochrome P450s, non-heme Fe^{II}/α-ketoglutarate-dependent oxygenases and different kinds of transferases among others.[21]

Recently, a putative CDPS gene cluster could be identified in the genome of the actinobacterium *Actinosynnema mirum* using known CDPS sequences as BLAST queries.[20] Here, we describe the bioinformatic analysis of this CDPS gene cluster and the elucidation of the biosynthetic pathway leading to two Sch 725418 analogues. Our studies identify Amir_4627 as the first CDPS that shows high substrate specificity generating only one main product. Additionally, it is the first CDPS family member that can form ditryptophan DKPs and the first prokaryotic CDPS whose main product constituents differ from the four amino acids that usually make up CDPS-dependent CDPs (Phe, Leu, Tyr, and Met). We show that after cWW formation a *S*-adenosyl-L-methionine (SAM)-dependent *N*-methyltransferase (Amir_4628) conducts two successive methylations at the DKP-ring nitrogens and additionally show that it is able to methylate four other CDPs. This makes Amir_4628 the first identified DKP-ring-modifying methyltransferase.

MATERIALS AND METHODS

General Methods and Instruments. High-performance liquid chromatography–tandem mass spectrometry (HPLC–MS^2) analyses of M9 fermentations were conducted using an Agilent 1100 HPLC system equipped with a Nucleodur C-18 ec column (125 mm × 4.6 mm, particle size of 3 μm, pore size of 110 Å, Macherey and Nagel, flow rate of 0.3 mL/min, solvent A consisting of 0.1% (v/v) TFA and dd-H_2O, solvent B consisting of 0.1% (v/v) TFA and acetonitrile, linear gradient from 0 to 95% over 50 min) connected to a Finnigan LTQ-FT Ultra instrument (Thermo Fischer Scientific). MS fragmentation experiments were conducted using collision-induced dissociation (CID) fragmentation. Preparative HPLC purification of scaled-up Amir_4628 assays was performed employing an Agilent 1100 Series HPLC system equipped with a Nucleodur C-18 ec column (250 mm × 21 mm, particle size of 5 μm, pore size of 110 Å, Macherey and Nagel, flow rate of 18 mL/min, solvent A consisting of 0.1% (v/v) TFA and dd-H_2O, solvent B consisting of 0.1% (v/v) TFA and acetonitrile, linear gradient from 0 to 95% over 50 min) and connected to a preparative scale fraction collector. HPLC–MS analyses of *in vitro* assays were conducted on an Agilent ESI-Quad 1100(A) Series MSD system equipped with a Nucleodur C-18 ec column (125 mm × 4.6 mm, particle size of 3 μm, pore size of 110 Å, Macherey and Nagel, flow rate of 0.3 mL/min, solvent A consisting of 0.1% (v/v) TFA and dd-H_2O, solvent B consisting of 0.1% (v/v) TFA and acetonitrile, linear gradient from 0 to 95% over 40 min). Nuclear magnetic resonance (NMR) spectra were recorded on a Bruker Avance 300 instrument with dimethyl sulfoxide-d_6 (Sigma-Aldrich) as

dx.doi.org/10.1021/bi4004827 | *Biochemistry* 2013, 52, 4274–4283

the solvent. Kinetic parameters were determined by using experimentally obtained starting velocities and the Enzyme Kinetic Module for Sigma Plot version 8.0 (SPSS).

Generation of Expression Constructs for Amir_4627, Amir_4628, and AlbC. The genes encoding Amir_4628 and AlbC were amplified by polymerase chain reaction (PCR) from genomic DNA of *A. mirum* (DSM 43827) and *S. noursei* (DSM 40635), respectively, obtained from DSMZ. The sequence of the putative CDP cluster found in *A. mirum*, containing the *Amir_4626*, *Amir_4627*, and *Amir_4628* genes, was optimized for *Escherichia coli* expression, synthesized, and cloned into the pMK-RQ vector by GeneArt (Life Technologies). The pMK-RQ vector was subsequently used for PCR amplification of different constructs. All PCR primers are listed in Table S1 of the Supporting Information. The *Amir_4628* gene was cloned into the first multiple cloning site of the pCDFDuet-1 vector, while *Amir_4627* and *albC* were cloned into the pET28a and pET41a vectors, respectively. After transformation of *E. coli* TOP10 cells (Invitrogen, Life Technologies), the resulting constructs were confirmed by sequencing (GATC-Biotech).

Production and Purification of Recombinant Proteins. The resulting expression constructs of Amir_4627 and Amir_4628 were used to transform *E. coli* BL21(DE3) cells (Novagen), which were grown at 37 °C to an OD_{600} of 0.6 and subsequently induced using isopropyl thiogalactopyranoside (IPTG, final concentration of 0.05 mM). Then the cultures were grown for 18 h at 18 °C and harvested via centrifugation (7000 rpm for 20 min at 4 °C). Cells were suspended in Tris buffer A [100 mM Tris, 300 mM NaCl, 10 mM β-mercaptoethanol, and 5% glycerol (pH 8)] and lysed with a French press (SLM Aminco, Thermo French press). The soluble lysate was separated from cell debris by centrifugation (17000 rpm for 30 min at 4 °C), filtered through a 0.2 μm Filtropur S filter (Sarstedt), and then subjected to Ni-NTA affinity purification using an Äkta Prime system (GE Healthcare Life Sciences). After equilibration of the Ni-NTA column with Tris buffer A and application of the lysate, the bound protein was eluted using gradient elution with an increasing imidazole concentration (from 2 to 95% over 30 min). Protein-containing fractions were identified by sodium dodecyl sulfate−polyacrylamide gel electrophoresis (SDS−PAGE), combined, and in the case of Amir_4627 subjected to heparin affinity chromatography using a HiTrap Heparin HP column (GE Healthcare Biosciences). Amir_4627 was eluted employing a linear salt gradient (from 0.3 to 2 M NaCl). Designated protein fractions were identified by SDS−PAGE and combined. The chromatographic step using a Heparin HP column was omitted from the purification protocol of Amir_4628. After the one-step (Amir_4628) or two-step (Amir_4627) purification procedure, protein-containing fractions were subjected to buffer exchange using Tris dialysis buffer [100 mM Tris, 50 mM NaCl, 10 mM β-mercaptoethanol, and 5% glycerol (pH 7.5)] with a HiPrep desalting column (GE Healthcare Life Sciences). Protein-containing fractions were pooled, concentrated, and flash-frozen using liquid N_2 before being stored at −80 °C until further use.

***In Vivo* Characterization of Amir_4627.** Preparatory cultures of cells containing the Amir_4627 expression construct were used to inoculate [1:50 (v/v)] M9 minimal medium [17 g/L $Na_2HPO_4{\cdot}12H_2O$, 3 g/L KH_2PO_4, 0.5 g/L NaCl, 1 g/L NH_4Cl, a 1 mL/L $MgSO_4$ solution (2 M), a 0.2 mL/L $CaCl_2$ solution (0.5 M) (pH 7.0), a 10 mL/L glucose solution (40%, w/v), and a 0.2 mL/L vitamin mix (Table S2 of the Supporting Information) after autoclaving]. M9 cultures were grown at 37 °C to an OD_{600} of 0.6 and subsequently induced using IPTG (final concentration of 0.05 mM). After incubation at 18 °C for 18 h, cultures were harvested through centrifugation (17000 rpm for 20 min at 4 °C), filtered through a 0.2 μm Filtropur S filter, and subjected to HPLC−MS^2 analysis. Produced amounts of cWW were estimated using an authentic standard (Bachem).

Determination of the cWW Stereoconfiguration. The absolute stereoconfiguration of cWW was determined by acid hydrolysis of the DKP followed by chiral HPLC analysis and comparison with authentic standards of D-/L-Trp; 500 μg of cWW was hydrolyzed by the addition of 200 μL of 6 M HCl and incubation at 95 °C for 24 h. After neutralization using 10 M NaOH, the sample was subjected to chiral HPLC analysis (Phenomenex, Chirex3126, 250 mm × 4.6 mm, particle size of 5 μm, pore size of 110 Å, flow rate of 1 mL/min, solvent A consisting of 2 mM $CuSO_4$ in dd-H_2O, solvent B consisting of methanol) using isocratic conditions (30% B).

***In Vitro* Characterization of Amir_4627.** In a typical Amir_4627 assay, recombinant Amir_4627 (10 μM) was incubated with 50 μM tRNA mix from *Saccharomyces cerevisiae* (Sigma-Aldrich), *E. coli* aminoacyl-tRNA synthetase mix (250 units, Sigma-Aldrich), and different amino acids (1 mM) at 30 °C. Additionally, the assay contained ATP (500 μM), $MgCl_2$ (10 mM), KCl (30 mM), and DTT (2 mM) in Tris buffer [50 mM Tris and 300 mM NaCl (pH 7.5)]. The reactions were stopped by the addition of TCA [final concentration of 5% (v/v)] and subjected to HPLC−MS analysis.

***In Vivo* Characterization of Amir_4628.** M9 fermentations of *E. coli* BL21(DE3) cells transformed with both Amir_4627 and Amir_4628 or AlbC and Amir_4628 were conducted in a manner analogous to that of the Amir_4627 fermentations described above. To ensure reproducibility of Amir_4627/Amir_4628 and AlbC/Amir_4628 fermentations, the expression constructs of Amir_4627 and Amir_4628 were constructed in a way that they carried both compatible selection marker genes and compatible origins of replication (Amir_4627/AlbC, kanamycin, f1; Amir_4628, spectinomycin, CDF).

***In Vitro* Characterization of Amir_4628.** For time course measurements, recombinantly produced Amir_4628 (20 μM) was incubated with 1 mM *S*-adenosyl-L-methionine and 1 mM cWW in Tris buffer [50 mM Tris and 300 mM NaCl (pH 7.5)]. Reactions were stopped by the addition of TCA [final concentration of 5% (v/v)] and mixtures subjected to HPLC−MS analysis.

The kinetic parameters of the second Amir_4628 methylation step were determined by varying the concentration of purified cWW-Me from 0 to 1 mM while keeping the SAM and enzyme concentrations constant. Assays were initiated by the addition of Amir_4628 and stopped by adding TCA [final concentration of 5% (v/v)] after 8 min, which was determined to be an appropriate reaction time being in the linear conversion range. Samples were then subjected to HPLC−MS analysis.

Purification of cWW-Me for Use in Amir_4628 Kinetic Analysis. Amir_4628 assays were scaled up, stopped after 20 min, which was determined to be the most appropriate reaction time for maximizing the cWW-Me yield, and subsequently subjected to preparative HPLC purification. Product fractions were combined, flash-frozen using liquid N_2, and lyophilized. The resulting products were stored at −20 °C until further use (Figure S1 of the Supporting Information).

Antibacterial Activity Assays of cWW, cWW-Me, and cWW-Me_2. Antibacterial activities were evaluated against bacterial strains *E. coli* BL21(DE3), *Bacillus subtilis* MR168,

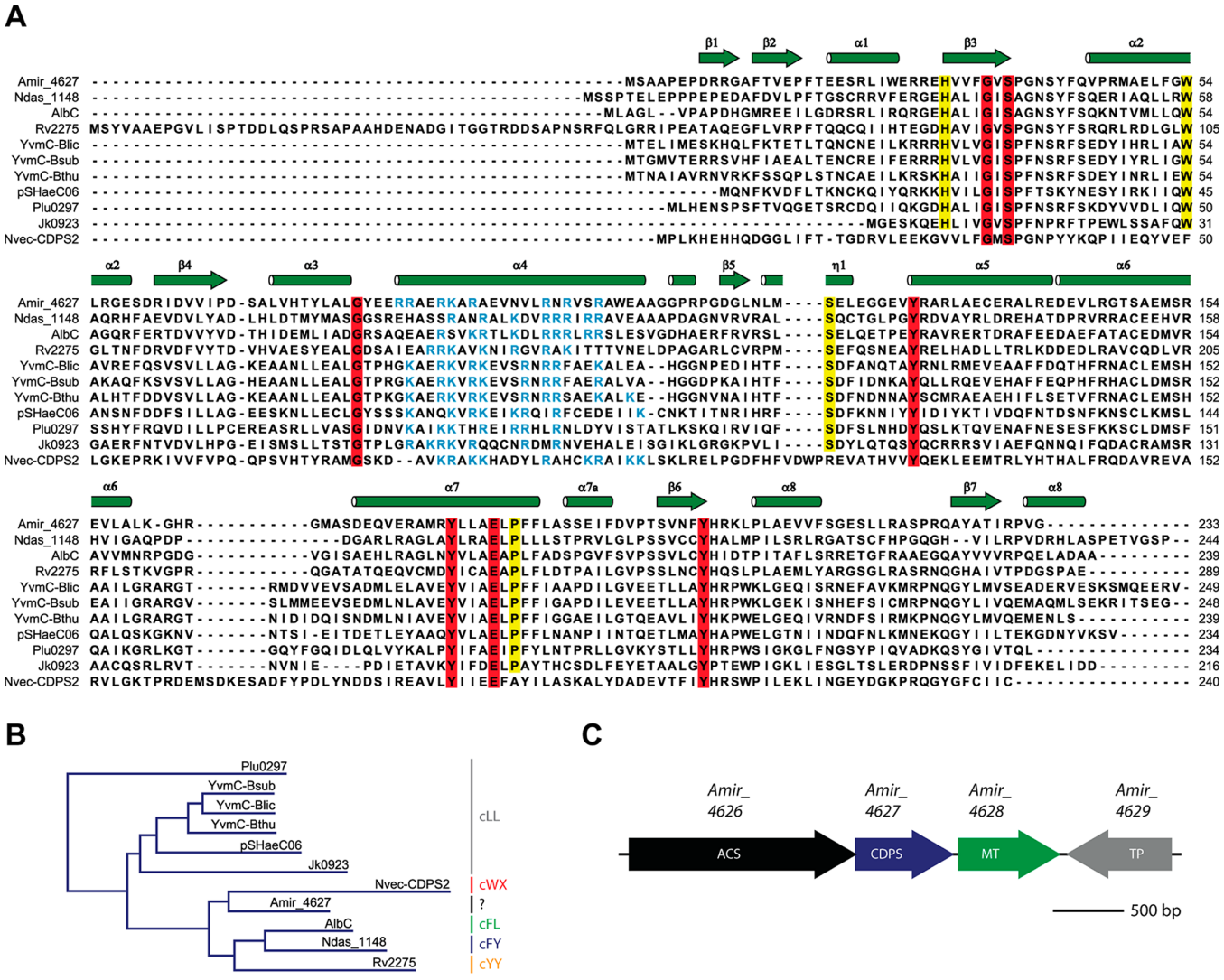

Figure 2. Bioinformatic analysis of the *A. mirum* CDPS gene cluster. (A) Multiple-sequence alignment of known CDPSs and Amir_4627. The secondary structural elements of AlbC are colored green above the alignment. Residues conserved in all characterized CDPSs are highlighted with a red background, while residues conserved in all prokaryotic members are highlighted with a yellow background. The positively charged residues in helix α4 proposed to mediate protein−tRNA interactions are colored blue. (B) Phylogenetic tree based on the multiple-sequence alignment shown in panel A with the respective CDPS main products. The product shown for Ndas_1148 is based on studies currently conducted by our group. (C) *A. mirum* CDPS gene cluster with the truncated IS4 transposase gene located directly downstream of Amir_4628. Abbreviations: ACS, acyl-CoA ligase; MT, methyltransferase; TP, transposase.

and *Micrococcus flavus* ATCC 10240 using spot-on-lawn assays on LB (lysogeny broth). Soft agar was prepared by adding 0.7% agar to liquid LB. Soft agar (10 mL) was then inoculated using 100 μL of an overnight culture of the respective organism and spread evenly on an LB agar plate. Next, 10 μL of the respective compound and dilution (1, 10, and 100 μg/mL cWW, cWW-Me, and cWW-Me$_2$) was spotted on the soft agar plate followed by overnight incubation at 30 °C.

RESULTS

Bioinformatic Analysis of a Putative CDP Biosynthetic Gene Cluster in *A. mirum*. A bioinformatic survey in 2010 first identified a putative CDPS gene (*Amir_4627*) in *A. mirum* using AlbC (the prototypical CDPS) and other characterized CDPS family members as queries in iterative PSI-BLAST searches.[20] The sequence of the identified gene product, annotated as a "hypothetical protein", is 33% identical and 46% similar to that of AlbC, which is in accordance with the only moderate level of sequence identity and similarity of characterized CDPSs among each other. To further investigate if Amir_4627 is a functional CDPS, a Clustal Omega[23,24] multiple-sequence alignment with known CDPSs was generated. This analysis shows that the active-site nucleophile Ser36 (β3), 11 other positions usually conserved in prokaryotic CDPSs, and the positively charged helix (α4) proposed to mediate tRNA binding during enzyme catalysis are all well-preserved in Amir_4627 (Figure 2A).

Using the protein threading and fold recognition server I-TASSER,[25,26] a structural model of Amir_4627 was generated on the basis of the crystal structure of the CDPS YvmC from *Bacillus licheniformis* as a template (Figure S2 of the Supporting Information).[27] The quality of a predicted structure can generally be judged by inspecting the respective TM score of a structural model and the root-mean-square deviation (rmsd) of the C_α atoms between the generated model and template. The TM score for the Amir_4627 model is 0.93 ± 0.06, indicating a correctly predicted overall topology and a high degree of

dx.doi.org/10.1021/bi4004827 | *Biochemistry* 2013, 52, 4274−4283

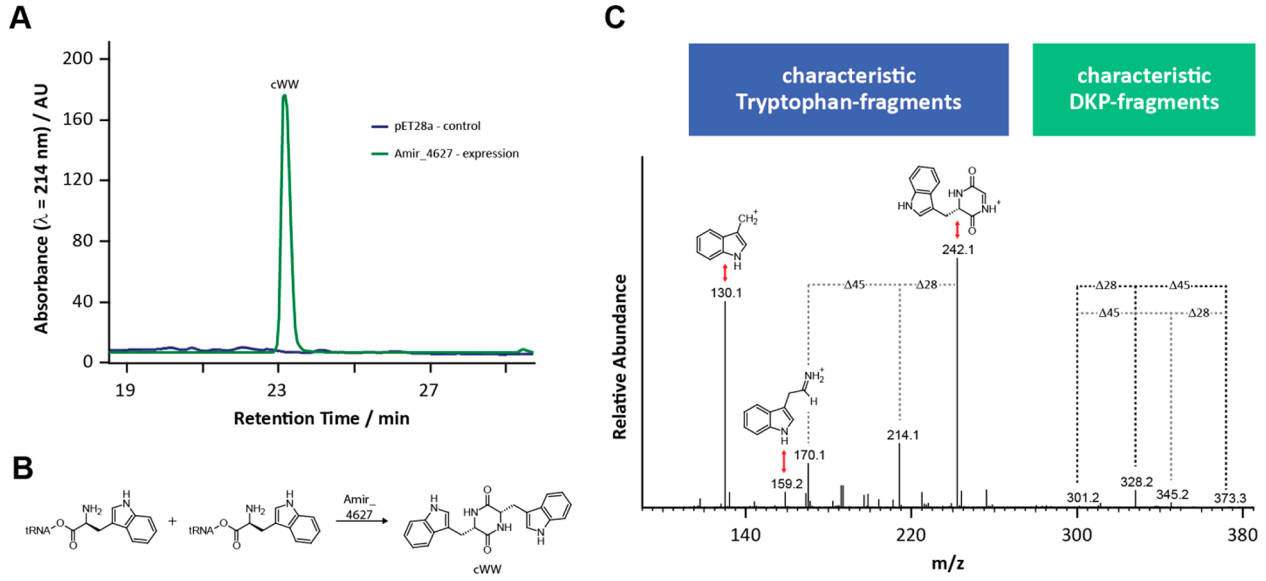

Figure 3. HPLC–MS analysis and product identification of the CDPS Amir_4627. (A) UV traces for Amir_4627 and the empty vector control of M9 fermentations. (B) Reaction catalyzed by Amir_4627 identified as a functional CDPS family member. (C) MS^2 fragmentation spectrum of cWW (m/z 373). Relevant fragment ions and neutral losses used to identify the CDPS Amir_4627 reaction product are shown.

structural homology to the template, which is additionally confirmed by the low rmsd of 2.6 ± 1.9 Å (over 215 C_α atoms). Taken together, those *in silico* results suggest that Amir_4627 is indeed a CDPS family member.

On the basis of the constructed multiple-sequence alignment, a phylogenetic tree was generated using the neighbor joining method (Figure 2B). The tree shows that all CDPSs that form cLL as a main product cluster together, while all other characterized CDPSs can be found in a separate clade. This expectedly reflects the evolutionary relationship of the respective producing organisms with cLL-producing species belonging to the phyla proteobacteria and firmicutes (except for JK0923 originating from the actinobacterium *Corynebacterium jeikeium*) and the remaining organisms being part of the phylum actinobacteria (except for Nvec-CDPS2 originating from the eukaryotic cnidarian *Nematostella vectensis*). The CDPS in question, Amir_4627, can be found in the lower main clade, interestingly with Nvec-CDPS2 as its closest relative.

With respect to the genetic surroundings of *Amir_4627*, a gene annotated as an "AMP-dependent synthetase and ligase" belonging to the family of long-chain fatty acyl-CoA ligases (*Amir_4626*) is located directly upstream of *Amir_4627* while a gene encoding a "CheR-type methyltransferase" (*Amir_4628*) can be found directly downstream of *Amir_4627*. It is possible that one or both of those genes are part of a dedicated CDP biosynthetic pathway. Additionally, a truncated transposase of the IS4 family (*Amir_4629*) is located directly downstream of *Amir_4628*, which could indicate that the *A. mirum* CDPS gene cluster described above was acquired through horizontal gene transfer (Figure 2C).

Amir_4627 Represents a Highly Specific CDPS Generating Exclusively cWW. To investigate the ability of Amir_4627 to synthesize DKPs, a heterologous expression approach was used in which *E. coli*, harboring an Amir_4627 expression construct, was cultivated in M9 minimal medium. This approach followed previous studies reporting that when a functional CDPS is heterologously produced in *E. coli* the generated DKPs can be identified directly in the culture supernatant.[17] Initial attempts to clone the native *Amir_4627* gene from *A. mirum* into pET28a were successful, but after IPTG induction, no protein production could be detected under various expression conditions. To circumvent this problem, an *E. coli* optimized synthetic version of the *Amir_4627* gene that could again be successfully cloned into pET28a and subsequently introduced into *E. coli* BL21(DE3) was used. Using this optimized expression construct, the encoded CDPS could be successfully produced, and subsequent HPLC–MS analysis of overnight M9 fermentation supernatants and comparison with an empty vector control confirmed the presence of one additional major peak in the Amir_4627 UV trace (Figure 3A). HR-MS analysis showed that the identified peak belongs to a compound with an m/z of 373.1658. Checking against the masses of all possible DKPs resulting from the condensation of two proteinogenic amino acids, we found the experimentally determined mass corresponds well to the mass of cWW (m/z 373.1659) (Figure 3B). This assumption could be confirmed by detailed HPLC–MS^2 studies (Figure 3C) and NMR spectroscopy (Table S3 and Figures S3–S8 of the Supporting Information). The fragmentation spectra clearly show the characteristic fragmentation pattern of a 2,5-DKP moiety with successive neutral losses of 28 Da (-CO) and 45 Da (-$HCONH_2$) or vice versa.[28] Additionally, five fragments characteristic of Trp, including the immonium ion (m/z 159), could be identified. The absence of any further fragment peaks in the MS^2 spectra characteristic of other amino acids and the comparison of ^1H and ^{13}C NMR spectra with literature data[12] confirm that the isolated compound is indeed cWW (yield of 29 mg/L of M9 supernatant). For the determination of the cWW stereoconfiguration, acid hydrolysis of the isolated compound followed by chiral HPLC analysis was conducted. As expected for a CDPS-dependent DKP, only L-Trp could be identified (Figure S9 of the Supporting Information). To investigate if the CDPS in question produces any other minor DKP products, we checked the HPLC–MS chromatograms for all possible DKPs resulting from proteinogenic amino acids, but no additional differential peaks could be identified.

Subsequently, *in vitro* studies using purified Amir_4627 were conducted to further investigate DKP formation with regard to

dx.doi.org/10.1021/bi4004827 | *Biochemistry* 2013, 52, 4274–4283

substrate specificity. Following a three-step purification procedure, active CDPS could be obtained with a yield of 0.7 mg/L of culture (Figure S10 of the Supporting Information). To provide aa-tRNAs as substrates in *in vitro* assays, they had to be generated *in situ* by using the respective amino acids, a tRNA mix isolated from *S. cerevisiae*, and a mixture of *E. coli* aminoacyl-tRNA synthetases. Different combinations of the amino acids usually found in DKPs produced by CDPSs were tested, but only when Trp was present could DKP formation be detected with cWW being the only observed product (Figure 4).

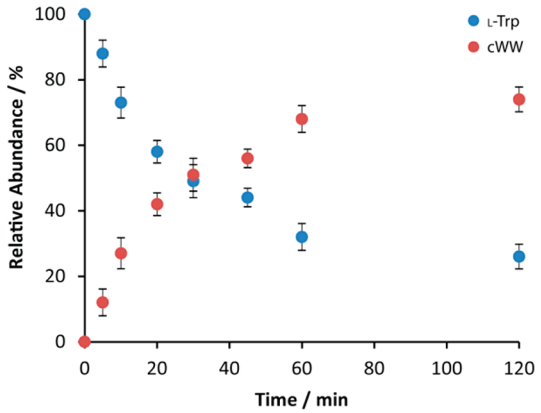

Figure 4. *In vitro* time course analysis of the CDPS-catalyzed formation of cWW.

The SAM-Dependent Methyltransferase Amir_4628 Is Able To Conduct N-Methylations at the DKP Core of Different CDPs. To investigate the potential of the putative methyltransferase Amir_4628 to modify DKPs in general and cWW in particular, we successfully cloned the respective native gene into pCDFDuet-1 and used it in M9 fermentation experiments. Subsequent HPLC–MS analysis of the M9 culture supernatants and comparison with empty vector and Amir_4627 controls confirmed the presence of two new differential peaks at later retention times (Figure 5). HR-MS analysis revealed the masses of the two compounds to correspond to m/z 387.1815 and 401.1971. Those are in good agreement with the masses expected for singly (cWW-Me; m/z 387.1815) and doubly (cWW-Me_2; m/z 401.1972) methylated cWW, respectively. To

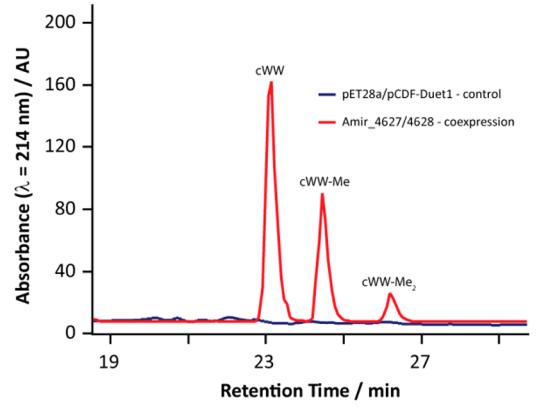

Figure 5. HPLC analysis of M9 culture supernatants resulting from cotransformation experiments using Amir_4627 and Amir_4628. UV traces of M9 supernatants from cultures transformed with both constructs and an empty vector control are shown.

confirm this assumption and to clarify the positions at which the methylations take place, detailed HPLC–MS^2 studies were conducted (Figure 6A). The resulting fragmentation spectra clearly show that the two new compounds both contain a 2,5-DKP moiety because of the characteristic neutral losses discussed above. Additionally, the presence of characteristic Trp fragments indicates that the two compounds are indeed cWW derivatives. To elucidate the positions at which methylation took place first, the increase and the decrease in the intensity of fragments corresponding to Trp (m/z 159) and putatively methylated Trp (m/z 173) immonium ions were analyzed. Via comparison of the fragmentation spectra of cWW, putative cWW-Me, and putative cWW-Me_2, it becomes obvious that in the case of cWW only unmethylated immonium ions (m/z 159) can be detected, while for putative cWW-Me, both methylated and unmethylated immonium ions can be found in equal amounts (m/z 173 and 159, respectively). In the case of putative cWW-Me_2, as expected, only methylated immonium ions (m/z 173) are present. Upon closer examination of the characteristic DKP fragmentation pattern, in the case of putative cWW-Me and cWW-Me_2 not only can the expected neutral losses of 28 (-CO) and 45 Da (-$HCONH_2$) be detected, but an additional neutral loss of 59 Da can be observed, which completely substitutes the neutral loss of 45 Da (-$HCONH_2$) in the case of putative cWW-Me_2. This neutral loss of 59 Da corresponds to a HCONHCH_3 fragment, indicating that a methylation took place in the DKP ring itself. Combining this fact with the detection of methylated immonium ions for cWW-Me and cWW-Me_2 and the NMR spectroscopic data leads to the conclusion that the only reasonable methylation positions are the two α-nitrogens of the 2,5-DKP moiety (Figure 6B).

To test the antibacterial activities of the three identified compounds (cWW, cWW-Me, and cWW-Me_2), we subjected them to spot-on-lawn assays using *E. coli* Bl21(DE3), *B. subtilis* MR168, and *M. flavus* ATCC 10240 at concentrations of $\leq$100 μg/mL. None of the tested compounds showed any significant antibacterial activity against the tested indicator strains.

For subsequent *in vitro* studies, the methyltransferase Amir_4628 was recombinantly produced in *E. coli* and purified with a yield of 2.5 mg/L of culture. A time course analysis of the methylations of cWW was conducted showing that two successive separate methylation steps take place where the first methylation product, cWW-Me, is released from the enzyme after the initial methylation reaction (Figure 7A). This can be deduced by the fact that large amounts of free cWW-Me can be observed during the Amir_4628-catalyzed reaction with a maximal relative amount of cWW-Me after an incubation time of ~20 min. After incubation for 60 min, formation of the final methylation product cWW-Me_2 has almost come to a halt, probably because of enzyme degradation because increased levels of enzyme precipitate could be observed using longer incubation times and methylation activity could be restored by adding fresh enzyme. To further characterize Amir_4628, methylation assays were scaled up, incubated for 20 min, at which time the largest amount of cWW-Me is present in the reaction mixture, and subjected to preparative HPLC purification. cWW-Me was then used as a substrate to determine the kinetics of the second methylation step (Figure 7B). For the methylation of cWW-Me, an apparent K_m of 51 $\pm$ 4 μM and a k_{cat} of 4.4 $\pm$ 0.13 min^{-1} were determined.

To further test the substrate specificity of the methyltransferase Amir_4628, M9 fermentations were conducted using *E. coli* BL21(DE3) cells transformed with both *albC* and *Amir_4628*.

dx.doi.org/10.1021/bi4004827 | *Biochemistry* 2013, 52, 4274–4283

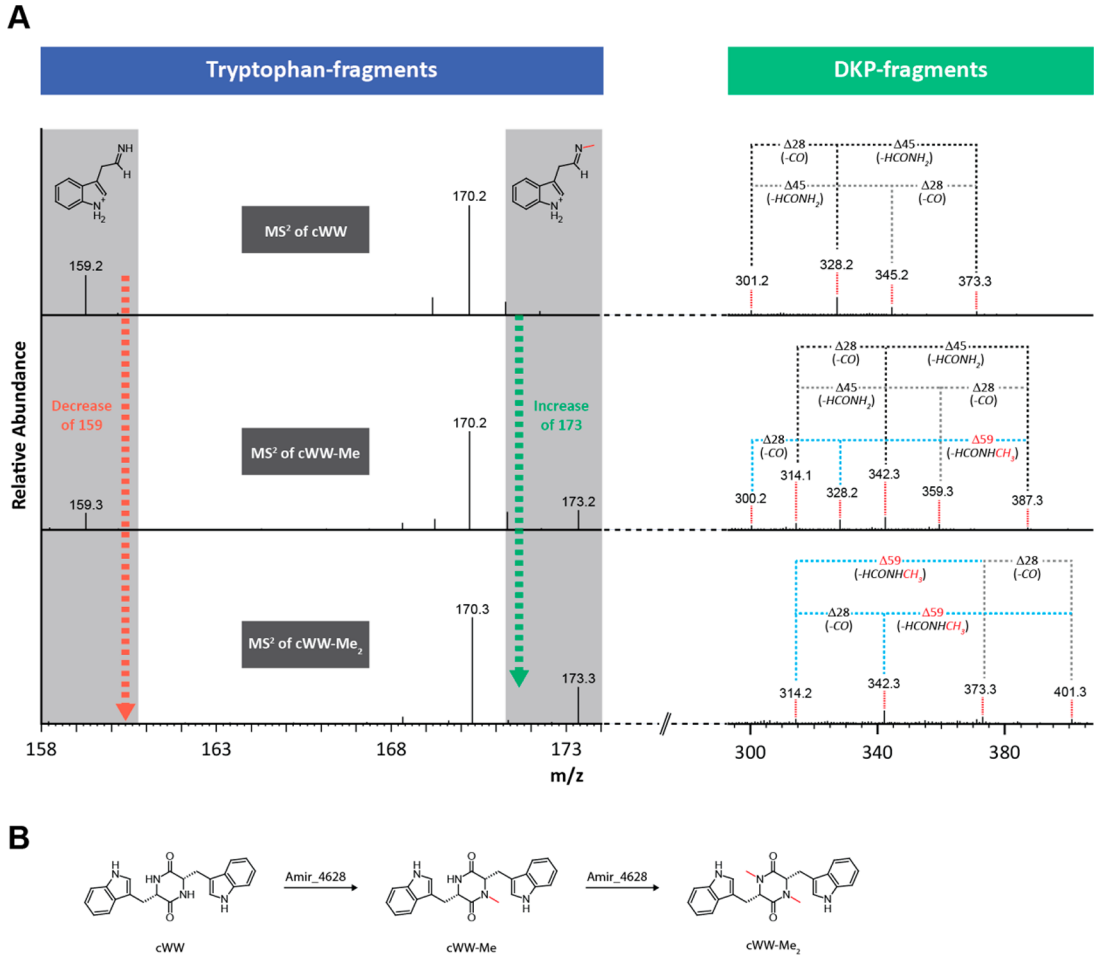

Figure 6. Elucidation of the regiochemistry of the investigated methylation reactions. (A) MS^2 fragmentation comparison of cWW, cWW-Me, and cWW-Me_2. On the left, the decrease and increase of unmethylated and methylated Trp immonium ions are shown. On the right, the differences in the characteristic 2,5-DKP fragmentation patterns between methylated and unmethylated cWW are shown. Series of neutral losses that are observed only in methylated cWW derivatives are highlighted in cyan. Neutral losses containing a newly installed methyl group are colored red. (B) Reaction sequence resulting in the formation of cWW-Me_2 catalyzed by Amir_4628. The newly installed methyl groups are colored red.

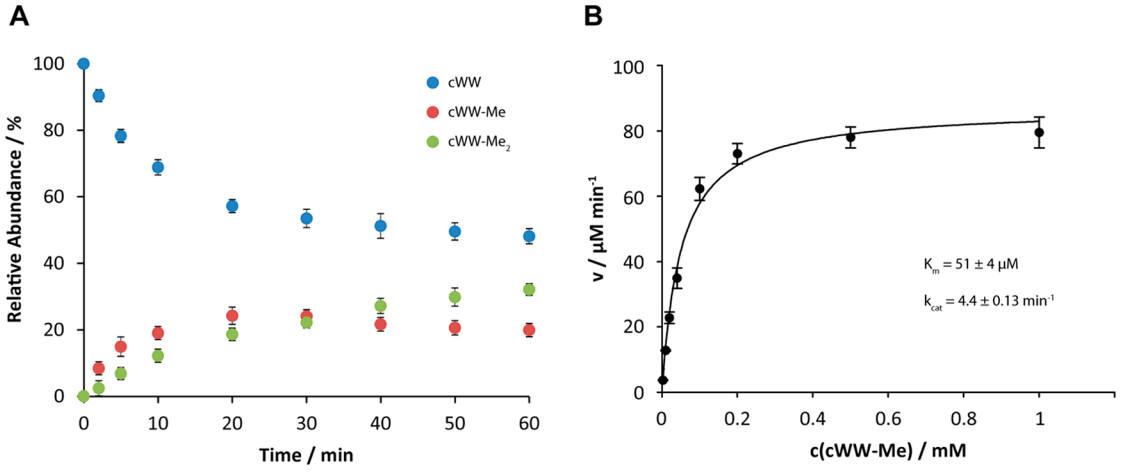

Figure 7. *In vitro* analysis of the methyltransferase Amir_4628. Error bars indicate standard errors of three independent experiments. (A) Time course for the two successive methylation reactions. (B) Kinetic characterization of the second methylation step and calculated kinetic parameters.

The CDPS AlbC has been previously characterized and was shown to produce all possible DKPs using the amino acids Phe, Leu, Tyr, and Met.[17] With this approach, it was possible to test Amir_4628 substrate specificity for 10 different DKPs in one experiment. Four DKPs could be shown to be valid substrates of Amir_4628 (cFF, cFL, cFY, and cFM), all containing at least one phenylalanine residue, with cFF-Me and cFF-Me_2 being the major methylation products (Table 1 and Figure S11 of the Supporting Information). The only other DKP besides cFF for which double methylation could be observed was cFY.

dx.doi.org/10.1021/bi4004827 | *Biochemistry* 2013, 52, 4274−4283

Table 1. Substrate Specificities of the Methyltransferase Amir_4628[a]

cXX	cXX-Me (relative amount)[b]	cXX-Me$_2$ (relative amount)[b]
cWW	68%	22%
cFF	31%	11%
cFY	4%	<1%
cFM	2%	–
cFL	2%	–

[a]Values obtained for relative production amounts are based on 18 h fermentations in M9 medium. [b]Relative amount compared to the respective cXX calculated using UV trace integrals.

DISCUSSION

Trp-containing CDPs are among the most common natural products harboring a 2,5-DKP moiety with a large majority of known compounds isolated from fungal sources. In bacteria, CDPs containing one Trp residue are also quite common, while only one example of a monocyclic ditryptophan DKP could be isolated so far, Sch 725418 (*Micromonospora* sp.).[12] Until now, neither a biosynthetic gene cluster nor a biochemical pathway for the generation of a monocyclic ditryptophan CDP has been reported.

Starting with the hypothesis that Amir_4627, recently identified in a bioinformatic survey, is a putative CDPS, we set out to further analyze Amir_4627 and the surrounding gene products initially using different *in silico* methods. The putative CDPS gene cluster contains two genes encoding candidate DKP-modifying enzymes (Amir_4626 and Amir_4628) located directly up- and downstream of *Amir_4627* (Figure 2C). Together, those three genes span approximately 2.9 kb, not including the truncated IS4 transposase located directly downstream of the gene encoding the methyltransferase *Amir_4628*. The presence of a transposase gene may indicate that *A. mirum* has acquired this particular CDPS gene cluster via horizontal gene transfer, which is supported by the fact that a highly similar gene cluster with an identical genetic organization is present in its close relative *Streptomyces* sp. AA4 (Figure S12 of the Supporting Information). We turn now to the two putative CDP tailoring enzymes Amir_4626 and Amir_4628, which are annotated as a long-chain fatty acyl-CoA ligase and a CheR-type methyltransferase, respectively. The fatty acyl-CoA ligase family catalyzes a two-step process in which a fatty acid is initially activated as an adenylate, which is then attacked by CoA to form a fatty acyl-CoA product. Generally, this activated fatty acid is then transferred onto a specific nucleophile through the action of an acyl-CoA transferase. No such transferase is encoded in the vicinity of Amir_4626, raising the question of the function it could play in CDP biosynthesis, which will be further addressed below.

Our initial assumption that Amir_4627 belongs to the CDPS family was proven to be correct through a combination of *in vivo* and *in vitro* analyses. It could be shown that Amir_4627 is able to produce a single DKP product, cWW (Figures 3 and 4). This high substrate specificity as well as the identity of the product is unusual for CDPSs. So far, all reported CDPS family members possess relaxed substrate specificities producing between 2 and 13 different DKPs.[17,22] Additionally, the identity of the DKP constituents of the Amir_4627 product is unusual because all known prokaryotic CDPSs produce DKPs consisting of different combinations of the amino acids Phe, Leu, Tyr, and Met, while the only characterized CDPS of eukaryotic origin additionally generates Trp-containing CDPs, but not cWW. The fact that the CDPS Amir_4627 produces only a single product contradicts the notion that the characteristic product profiles observed for most CDPSs result from a high specificity for the first aminoacyl-tRNA substrate and a relaxed specificity for the second aminoacyl-tRNA. On the contrary, it seems that in the case of Amir_4627 the second step is also highly specific. With regard to the specificity of the first incorporated amino acid, it was previously proposed that by comparing the residues lining the CDPS substrate pocket some general rules governing substrate specificity in CDPS catalysis could be deduced. For the cWX-producing CDPS Nvec-CDPS2 from *N. vectensis*, it was suggested that the specificity for Trp resulted from the presence of a large number of aromatic residues in the active site pocket (F61, Y194, and F209), which would supposedly facilitate Trp binding through π-interactions with the indole side chain.[22] Using a structure-based alignment, a comparison of the active site residues of all characterized CDPSs was generated (Table S4 of the Supporting Information) showing that at the corresponding three positions in Amir_4627 only one aromatic amino acid can be found (V65, F184, and N199). Via comparison of this active site with those of CDPSs of other specificities, it seems obvious that no easy prediction about the identity of the first incorporated amino acid, solely based on the active site residues, can be made. The high specificity of the second reaction step in Amir_4627 catalysis seems to be governed by an as yet unknown mechanism. This topic could be addressed in future studies through cocrystallization experiments with CDPS and an appropriate aminoacyl-tRNA analogue.

Turning now to the two putative DKP-modifying enzymes located in the *A. mirum* CDPS cluster, we could not assign a function to Amir_4626 annotated as a fatty acyl-CoA ligase. Neither *in vivo* fermentation experiments using all three genes (*Amir_4626*, *Amir_4627*, and *Amir_4628*) in their native organization nor *in vitro* studies of the recombinant protein led to the detection of any reaction products of Amir_4626. This could be explained by the absence of the correct fatty acid substrate in the heterologous host and the *in vitro* assays (C12:0, C14:0, C16:0, and C18:0 fatty acids were the substrates tested). Additionally, the absence of a dedicated acyl-CoA transferase in the *A. mirum* CDPS gene cluster makes it possible that even if the correct fatty acid substrate was present in *E. coli*, the Amir_4626 product could not be transferred onto its dedicated nucleophile. The second putative tailoring enzyme located directly downstream of the *Amir_4627* gene is Amir_4628 annotated as a CheR-type methyltransferase. With respect to the occurrence of different putative DKP-tailoring enzymes in CDPS gene clusters, by far the most common group consists of various kinds of oxidoreductases, including cytochrome P450s, non-heme Fe^{II}/α-ketoglutarate-dependent oxygenases, and other flavin- or pyridoxal phosphate-dependent oxidases.[21,29,30] On the other hand, only four organisms besides *A. mirum* in which methyltransferase genes are closely associated with putative CDPS genes are known, namely *Nocardiopsis dassonvillei* (two MTs), *Nocardiopsis alba* (two MTs), the organism encoding a CDPS cluster highly similar to that found in *A. mirum* mentioned above [*Streptomyces* sp. AA4 (one MT)] and *Kutzneria* sp. 744 (two MTs). The four *Nocardiopsis* MTs (currently under investigation in our group) all belong to the PF00891 family that includes various small molecule *O*-methyltransferases, among them DnrK (*Streptomyces peucetia*) and RdmB (*Streptomyces purpurascen*), which conduct different O-methylations at the anthracycline scaffold,[31,32] as well as various caffeic acid and isoflavone *O*-methyltransferases. One of the *Kutzneria*

dx.doi.org/10.1021/bi4004827 | *Biochemistry* 2013, 52, 4274−4283

MTs belongs to the largely uncharacterized PF04672 family that includes human histamine *N*-methyltransferase,[33] while the other mentioned MTs, including Amir_4628, are part of the PF01739 family. Among the members of the PF01739 family, different protein glutamate *O*-methyltransferases can be found as well as ToxA (*Burkholderia glumae*), which conducts N-methylations in toxoflavin biosynthesis.[34] The structure of toxoflavin consists of fused pyrimidinedione and 1,2,4-triazine rings in which one nitrogen in each ring is methylated through the action of ToxA. This specificity may indicate that Amir_4628 also acts as a *N*-methyltransferase on a six-memberd nitrogen-containing heterocyclic substrate. This hypothesis could indeed be proven right. In this study, we were able to show that Amir_4628 catalyzes two successive N-methylations at the 2,5-DKP core of five different CDPs. The position of methylation was investigated via HPLC−MS^2 studies in which both the characteristic neutral losses of the 2,5-DKP scaffold and methylated and unmethylated immonium ions were used to elucidate the exact regiospecificity of the Amir_4628-catalyzed reactions. The native substrate of Amir_4628 is cWW because it is the only DKP produced by the associated CDPS Amir_4627. The four other substrates accepted by Amir_4628, discovered through *in vivo* fermentation experiments using the formerly characterized promiscuous CDPS AlbC, are cFF, cFY, cFM, and cFL, listed in order of methylation efficiency. This indicates that Amir_4628 prefers DKPs containing large aromatic amino acids. Additionally, only substrates containing two aromatic amino acids could be doubly methylated (cWW, cFF, and cFY), suggesting that only α-nitrogens of aromatic amino acids are valid substrates for Amir_4628. It seems that the planar and aromatic nature of those substrates plays an important role in substrate recognition and/or catalysis. Kinetic analysis of the second methylation step catalyzed by Amir_4628 shows that its apparent K_m is approximately an order of magnitude larger than that for other CheR-type methyltransferases (protein-glutamate/aspartate *O*-methyltransferases), probably reflecting the difference between the interaction with a small molecule substrate and a larger protein surface. However, the turnover numbers are comparable.[35−37]

A large number of different modifying enzymes are known to originate from bacterial and especially fungal sources that use Trp-containing DKPs as substrates. Those include various varieties of prenyltransferases with different chemo- and regiospecificities, hydroxylases and other oxidoreductases modulating the oxidation state of the indole side chain, and various other enzymes triggering, for example, the formation of annulated Trp-containing DKPs. Many of the modifications introduced by those enzymes significantly influence the biological activity of the respective CDPs through the alteration of the hydrophobicity, shape, or rigidity of the natural product scaffold. The discovery of a potent catalyst for cWW formation encoded by a small gene opens the possibility for combinatorial *in vivo* as well as chemoenzymatic approaches in which different tailoring enzymes known to act upon Trp-containing DKPs can be used to generate derivatives of known natural products or entirely new chemical entities with potentially improved or new biological activities.

■ ASSOCIATED CONTENT

Ⓢ Supporting Information

Primers used in this study, M9 minimal medium vitamin mix, table of chemical shifts, and ^1H and ^{13}C NMR spectra of cWW, cWW-Me, and cWW-Me_2, sequence of the *E. coli*-optimized *Amir_4627* gene, comparison of CDPS active site residues, purification of cWW-Me via HPLC, structural models of Amir_4627, AlbC, and Nvec-CDPS2, chiral HPLC chromatogram of cWW acid hydrolysis, SDS−PAGE gels of Amir_4627 and Amir_4628, HPLC−MS analysis of AlbC/Amir_4628 M9 culture supernatants, and comparison of CDPS clusters in *A. mirum* and *Streptomyces* sp. AA4. This material is available free of charge via the Internet at http://pubs.acs.org.

■ AUTHOR INFORMATION

Corresponding Author

*Department of Chemistry, Philipps-University Marburg, 35043 Marburg, Germany. E-mail: marahiel@staff.uni-marburg.de. Phone: +49 (0) 6421 28 25722. Fax: +49 (0) 6421 28 22191.

Funding

This work has been supported by the Deutsche Forschungsgemeinschaft and the LOEWE Center for Synthetic Microbiology (SYNMIKRO).

Notes

The authors declare no competing financial interest.

■ ACKNOWLEDGMENTS

We thank Dr. Uwe Linne for support regarding mass spectrometric analyses.

■ REFERENCES

(1) Cain, C. C., Lee, D., Waldo, R. H., III, Henry, A. T., Casida, E. J., Jr., Wani, M. C., Wall, M. E., Oberlies, N. H., and Falkinham, J. O., III (2003) Synergistic antimicrobial activity of metabolites produced by a nonobligate bacterial predator. *Antimicrob. Agents Chemother. 47*, 2113−2117.

(2) Magyar, A., Zhang, X., Kohn, H., and Widger, W. R. (1996) The antibiotic bicyclomycin affects the secondary RNA binding site of *Escherichia coli* transcription termination factor Rho. *J. Biol. Chem. 271*, 25369−25374.

(3) Waring, P., and Beaver, J. (1996) Gliotoxin and related epipolythiodioxopiperazines. *Gen. Pharmacol. 27*, 1311−1316.

(4) Yamazaki, Y., Tanaka, K., Nicholson, B., Deyanat-Yazdi, G., Potts, B., Yoshida, T., Oda, A., Kitagawa, T., Orikasa, S., Kiso, Y., Yasui, H., Akamatsu, M., Chinen, T., Usui, T., Shinozaki, Y., Yakushiji, F., Miller, B. R., Neuteboom, S., Palladino, M., Kanoh, K., Lloyd, G. K., and Hayashi, Y. (2012) Synthesis and structure-activity relationship study of antimicrotubule agents phenylahistin derivatives with a didehydropiperazine-2,5-dione structure. *J. Med. Chem. 55*, 1056−1071.

(5) Kanzaki, H., Yanagisawa, S., Kanoh, K., and Nitoda, T. (2002) A novel potent cell cycle inhibitor dehydrophenylahistin: Enzymatic synthesis and inhibitory activity toward sea urchin embryo. *J. Antibiot. 55*, 1042−1047.

(6) Borthwick, A. D. (2012) 2,5-Diketopiperazines: Synthesis, reactions, medicinal chemistry, and bioactive natural products. *Chem. Rev. 112*, 3641−3716.

(7) Ortiz-Castro, R., Diaz-Perez, C., Martinez-Trujillo, M., del Rio, R. E., Campos-Garcia, J., and Lopez-Bucio, J. (2011) Transkingdom signaling based on bacterial cyclodipeptides with auxin activity in plants. *Proc. Natl. Acad. Sci. U.S.A. 108*, 7253−7258.

(8) Li, J., Wang, W., Xu, S. X., Magarvey, N. A., and McCormick, J. K. (2011) Lactobacillus reuteri-produced cyclic dipeptides quench agr-mediated expression of toxic shock syndrome toxin-1 in staphylococci. *Proc. Natl. Acad. Sci. U.S.A. 108*, 3360−3365.

(9) Degrassi, G., Aguilar, C., Bosco, M., Zahariev, S., Pongor, S., and Venturi, V. (2002) Plant growth-promoting *Pseudomonas putida* WCS358 produces and secretes four cyclic dipeptides: Cross-talk with quorum sensing bacterial sensors. *Curr. Microbiol. 45*, 250−254.

(10) Holden, M. T., Ram Chhabra, S., de Nys, R., Stead, P., Bainton, N. J., Hill, P. J., Manefield, M., Kumar, N., Labatte, M., England, D., Rice, S., Givskov, M., Salmond, G. P., Stewart, G. S., Bycroft, B. W., Kjelleberg, S.,

and Williams, P. (1999) Quorum-sensing cross talk: Isolation and chemical characterization of cyclic dipeptides from *Pseudomonas aeruginosa* and other Gram-negative bacteria. *Mol. Microbiol. 33*, 1254−1266.
(11) Kozlovsky, A. G., Vinokurova, N. G., Adanin, V. M., Burkhardt, G., Dahse, H. M., and Grafe, U. (2000) New diketopiperazine alkaloids from *Penicillium fellutanum*. *J. Nat. Prod. 63*, 698−700.
(12) Yang, S. W., Chian, T. M., Terracciano, J., Loebenberg, D., Chen, G., Patel, M., Gullo, V., Pramanik, B., and Chu, M. (2004) Structure elucidation of a new diketopiperazine Sch 725418 from *Micromonospora* sp. *J. Antibiot. 57*, 345−347.
(13) Shiono, Y., Akiyama, K., and Hayashi, H. (1999) New Okaramine Congeners, Okamines J, K, L, M and Related Compounds, from *Penicillium simplicissimum* ATCC90288. *Biosci., Biotechnol., Biochem. 63*, 1910−1920.
(14) Gardiner, D. M., and Howlett, B. J. (2005) Bioinformatic and expression analysis of the putative gliotoxin biosynthetic gene cluster of *Aspergillus fumigatus*. *FEMS Microbiol. Lett. 248*, 241−248.
(15) Healy, F. G., Wach, M., Krasnoff, S. B., Gibson, D. M., and Loria, R. (2000) The txtAB genes of the plant pathogen *Streptomyces acidiscabies* encode a peptide synthetase required for phytotoxin thaxtomin A production and pathogenicity. *Mol. Microbiol. 38*, 794−804.
(16) Robbel, L., Knappe, T. A., Linne, U., Xie, X., and Marahiel, M. A. (2010) Erythrochelin: A hydroxamate-type siderophore predicted from the genome of *Saccharopolyspora erythraea*. *FEBS J. 277*, 663−676.
(17) Gondry, M., Sauguet, L., Belin, P., Thai, R., Amouroux, R., Tellier, C., Tuphile, K., Jacquet, M., Braud, S., Courcon, M., Masson, C., Dubois, S., Lautru, S., Lecoq, A., Hashimoto, S., Genet, R., and Pernodet, J. L. (2009) Cyclodipeptide synthases are a family of tRNA-dependent peptide bond-forming enzymes. *Nat. Chem. Biol. 5*, 414−420.
(18) Lautru, S., Gondry, M., Genet, R., and Pernodet, J. L. (2002) The albonoursin gene Cluster of S noursei biosynthesis of diketopiperazine metabolites independent of nonribosomal peptide synthetases. *Chem. Biol. 9*, 1355−1364.
(19) Sauguet, L., Moutiez, M., Li, Y., Belin, P., Seguin, J., Le Du, M. H., Thai, R., Masson, C., Fonvielle, M., Pernodet, J. L., Charbonnier, J. B., and Gondry, M. (2011) Cyclodipeptide synthases, a family of class-I aminoacyl-tRNA synthetase-like enzymes involved in non-ribosomal peptide synthesis. *Nucleic Acids Res. 39*, 4475−4489.
(20) Aravind, L., de Souza, R. F., and Iyer, L. M. (2010) Predicted class-I aminoacyl tRNA synthetase-like proteins in non-ribosomal peptide synthesis. *Biol. Direct 5*, 48.
(21) Belin, P., Moutiez, M., Lautru, S., Seguin, J., Pernodet, J. L., and Gondry, M. (2012) The nonribosomal synthesis of diketopiperazines in tRNA-dependent cyclodipeptide synthase pathways. *Nat. Prod. Rep. 29*, 961−979.
(22) Seguin, J., Moutiez, M., Li, Y., Belin, P., Lecoq, A., Fonvielle, M., Charbonnier, J. B., Pernodet, J. L., and Gondry, M. (2011) Nonribosomal peptide synthesis in animals: The cyclodipeptide synthase of *Nematostella*. *Chem. Biol. 18*, 1362−1368.
(23) Sievers, F., Wilm, A., Dineen, D., Gibson, T. J., Karplus, K., Li, W., Lopez, R., McWilliam, H., Remmert, M., Soding, J., Thompson, J. D., and Higgins, D. G. (2011) Fast, scalable generation of high-quality protein multiple sequence alignments using Clustal Omega. *Mol. Syst. Biol. 7*, 539.
(24) Goujon, M., McWilliam, H., Li, W., Valentin, F., Squizzato, S., Paern, J., and Lopez, R. (2010) A new bioinformatics analysis tools framework at EMBL-EBI. *Nucleic Acids Res. 38*, W695−W699.
(25) Roy, A., Kucukural, A., and Zhang, Y. (2010) I-TASSER: A unified platform for automated protein structure and function prediction. *Nat. Protoc. 5*, 725−738.
(26) Zhang, Y. (2008) I-TASSER server for protein 3D structure prediction. *BMC Bioinf. 9*, 40.
(27) Bonnefond, L., Arai, T., Sakaguchi, Y., Suzuki, T., Ishitani, R., and Nureki, O. (2011) Structural basis for nonribosomal peptide synthesis by an aminoacyl-tRNA synthetase paralog. *Proc. Natl. Acad. Sci. U.S.A. 108*, 3912−3917.
(28) Guo, Y. C., Cao, S. X., Zong, X. K., Liao, X. C., and Zhao, Y. F. (2009) ESI-MS^n study on the fragmentation of protonate cyclic-dipeptides. *Spectroscopy 23*, 131−139.
(29) Belin, P., Le Du, M. H., Fielding, A., Lequin, O., Jacquet, M., Charbonnier, J. B., Lecoq, A., Thai, R., Courcon, M., Masson, C., Dugave, C., Genet, R., Pernodet, J. L., and Gondry, M. (2009) Identification and structural basis of the reaction catalyzed by CYP121, an essential cytochrome P450 in *Mycobacterium tuberculosis*. *Proc. Natl. Acad. Sci. U.S.A. 106*, 7426−7431.
(30) Gondry, M., Lautru, S., Fusai, G., Meunier, G., Menez, A., and Genet, R. (2001) Cyclic dipeptide oxidase from *Streptomyces noursei*. Isolation, purification and partial characterization of a novel, amino acyl α,β-dehydrogenase. *Eur. J. Biochem. 268*, 1712−1721.
(31) Jansson, A., Koskiniemi, H., Mantsala, P., Niemi, J., and Schneider, G. (2004) Crystal structure of a ternary complex of DnrK, a methyltransferase in daunorubicin biosynthesis, with bound products. *J. Biol. Chem. 279*, 41149−41156.
(32) Jansson, A., Niemi, J., Lindqvist, Y., Mantsala, P., and Schneider, G. (2003) Crystal structure of aclacinomycin-10-hydroxylase, a S-adenosyl-L-methionine-dependent methyltransferase homolog involved in anthracycline biosynthesis in *Streptomyces purpurascens*. *J. Mol. Biol. 334*, 269−280.
(33) Rutherford, K., Parson, W. W., and Daggett, V. (2008) The histamine N-methyltransferase T105I polymorphism affects active site structure and dynamics. *Biochemistry 47*, 893−901.
(34) Shingu, Y., and Yoneyama, K. (2004) Essential regulator gene toxR for toxoflavin biosynthesis of *Burkholderia glumae*. *J. Gen. Plant Pathol. 70*, 108−114.
(35) Schubert, H. L., Blumenthal, R. M., and Cheng, X. (2003) Many paths to methyltransfer: A chronicle of convergence. *Trends Biochem. Sci. 28*, 329−335.
(36) Djordjevic, S., and Stock, A. M. (1997) Crystal structure of the chemotaxis receptor methyltransferase CheR suggests a conserved structural motif for binding S-adenosylmethionine. *Structure 5*, 545−558.
(37) Simms, S. A., and Subbaramaiah, K. (1991) The kinetic mechanism of S-adenosyl-L-methionine: Glutamylmethyltransferase from *Salmonella typhimurium*. *J. Biol. Chem. 266*, 12741−12746.